Electronic Supplementary Material (ESI) for Journal of Materials Chemistry A.

Supplementary Information

Hydroxide ion dependent α-MnO_2 enhanced via oxygen vacancies as the negative electrode for high-performance supercapacitors

Yucheng Chen, Chengbao Zhou, Gang Liu, Chenxia Kang, Lin Ma, Qiming Liu*

Key Laboratory of Artificial Micro- and Nano-structures of Ministry of Education, School of Physics and Technology, Wuhan University, Wuhan, 430072, China

*Corresponding author: qmliu@whu.edu.cn

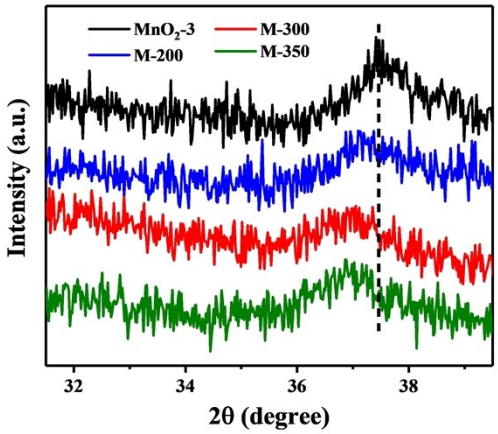

Fig.S1. The magnification of (211) peak.
(M-200: α-MnO_2 annealed at 200℃ for 3 h; M-350: α-MnO_2 annealed at 350℃ for 3 h)

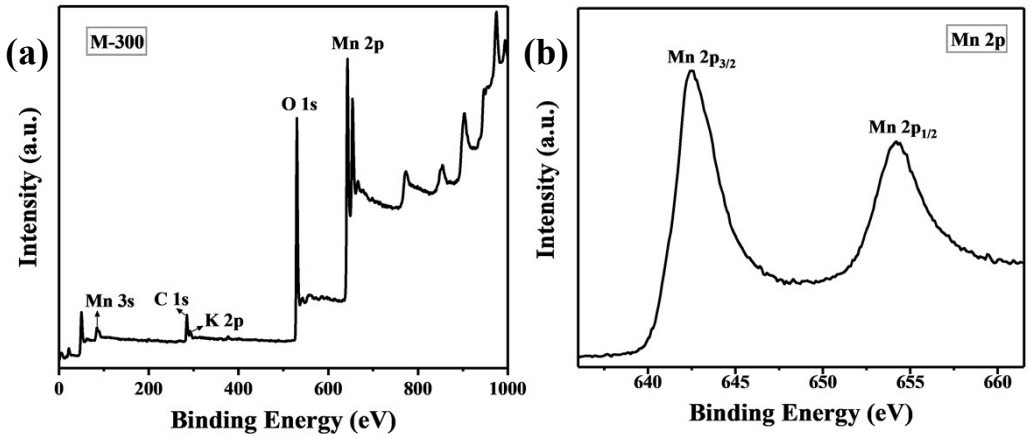

Fig.S2. (a) Data survey spectrum of M-300. (b) Mn 2p high resolution XPS spectra of M-300

Table S1. Atomic percentages of the elements in M-300 calculated from XPS survey spectra.

Element	Mn	O	K	C
Atomic %	28.31	51.38	4.80	15.51

Table S2. Binding energy and molar ratio of Mn and O element obtained from XPS results.

Element	Mn			O		
	Mn(IV)	Mn(III)	Mn(II)	O_{latt}	O_{ads}	O_{H_2O}
Binding energy (eV)	643.15	642.22	641.07	530.01	531.56	533.34
Molar ratio	1.00 ∶ 0.35 ∶ 0.11			1.00 ∶ 0.28 ∶ 0.06		

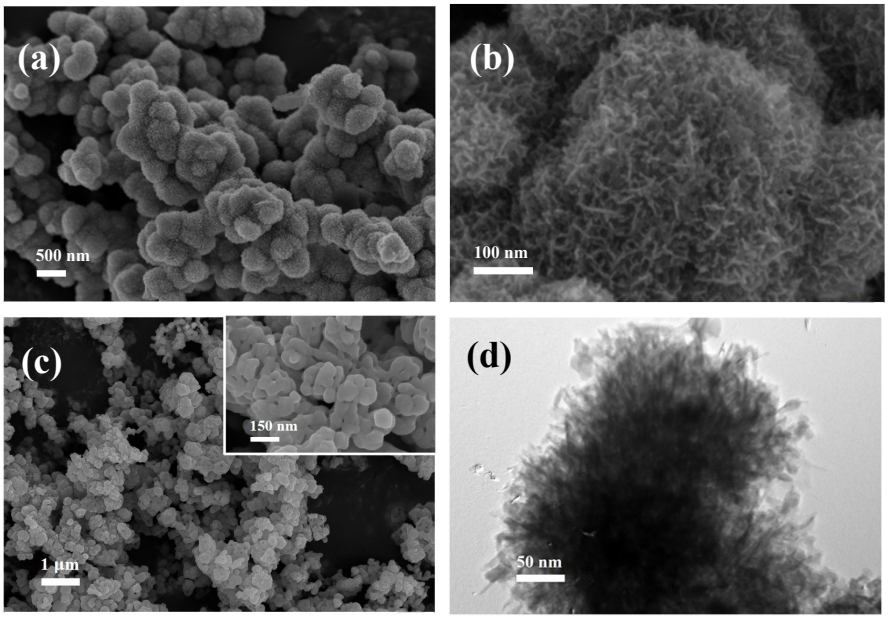

Fig.S3. SEM images of (a) M-200 and (c) M-700. (b) SEM enlarged image of M-200. (d) TEM image of MnO_2-3

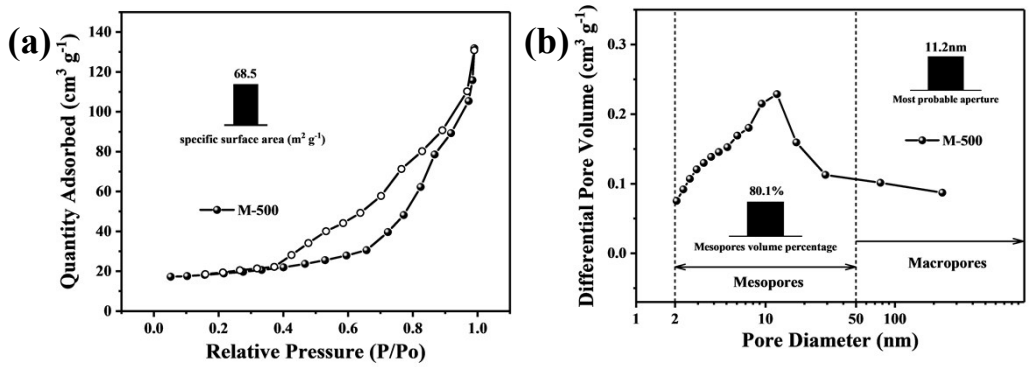

Fig.S4. (a) Nitrogen adsorption-desorption isotherm and (b) pore size distribution of M-500.

Table S3. Specific surface area and pore volume of all samples

Sample	Specific surface area (m^2 g^{-1})	Pore volume (cm^3 g^{-1})
MnO_2-1	33.6	0.168
MnO_2-2	77.7	0.217
MnO_2-3	115.7	0.249
M-300	119.5	0.311
M-500	68.5	0.159
M-700	64.9	0.144

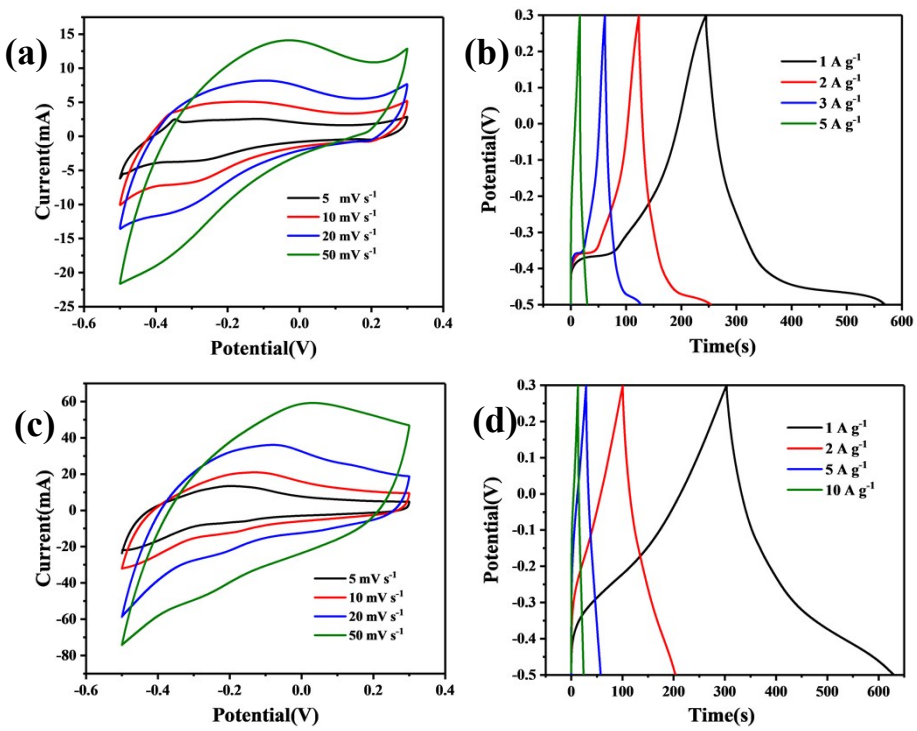

Fig.S5. CV curves of (a) MnO_2-1 and (c) MnO_2-2, GCD curves of (b) MnO_2-1 and (d) MnO_2-2

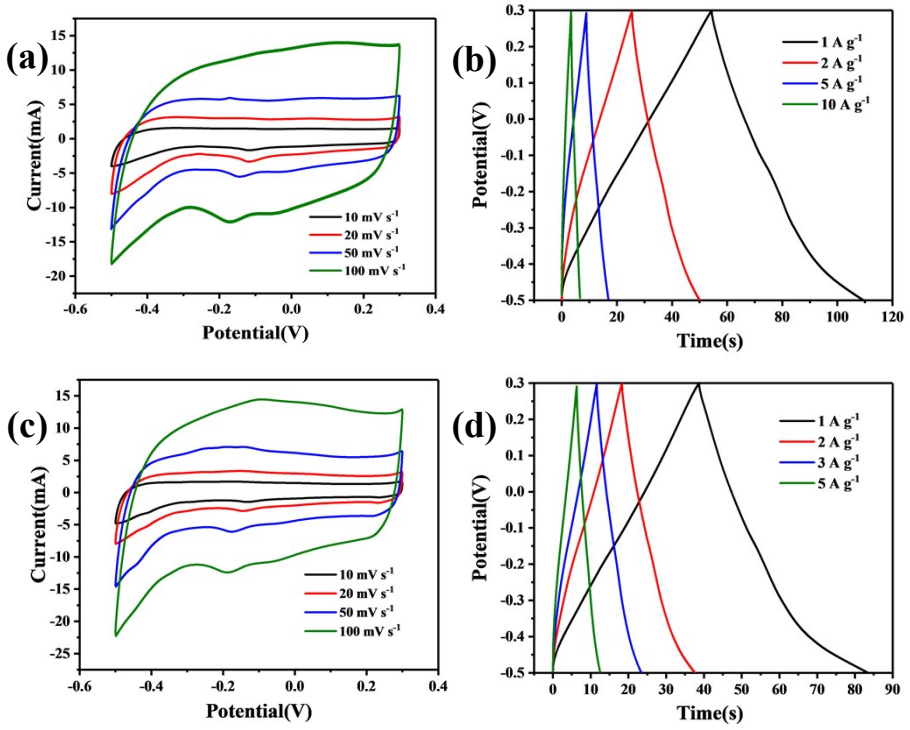

Fig.S6. CV curves of (a) M-500 and (c) M-700, GCD curves of (b) M-500 and (d) M-700

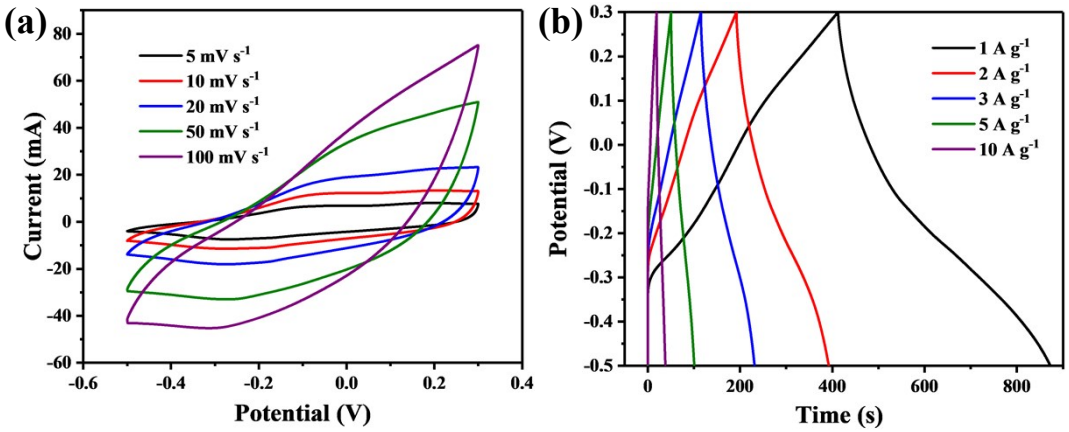

Fig.S7. (a) CV and (b) GCD curves of M-300 after 10,000 cycles

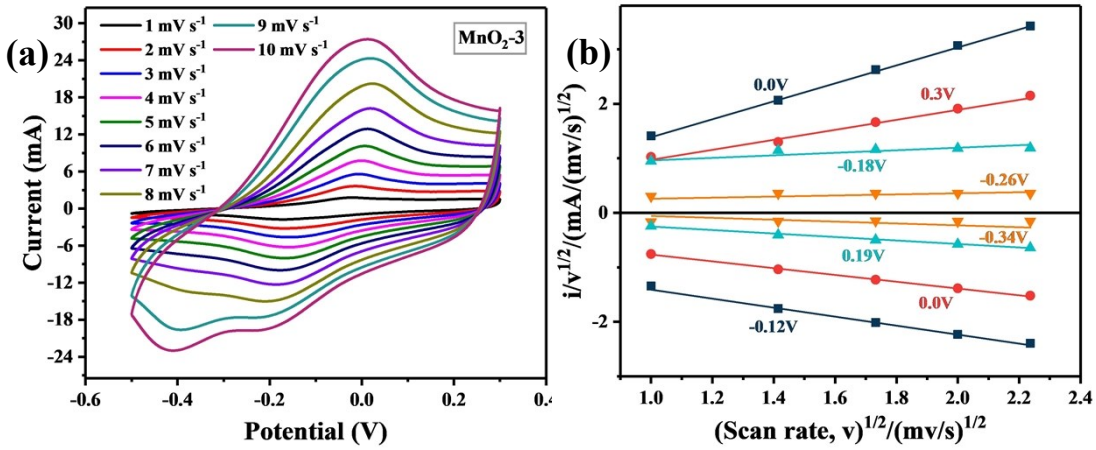

Fig.S8. (a) CV curves of MnO_2-3 at different scan rates. (b) The $v^{1/2}$ vs. $i/v^{1/2}$ curves of M-300 used to calculate the constants k_1 and k_2 at different potentials.

Table S4. Percentage of capacitance contribution of MnO_2-3 and M-300 at different scan rates

Sample	scan rate (mV s^{-1})				
	1.0	2.0	3.0	4.0	5.0
MnO_2-3	89.6%	93.7%	96.8%	98.3%	99.1%
M-300	78.7%	87.4%	93.4%	96.8%	98.8%

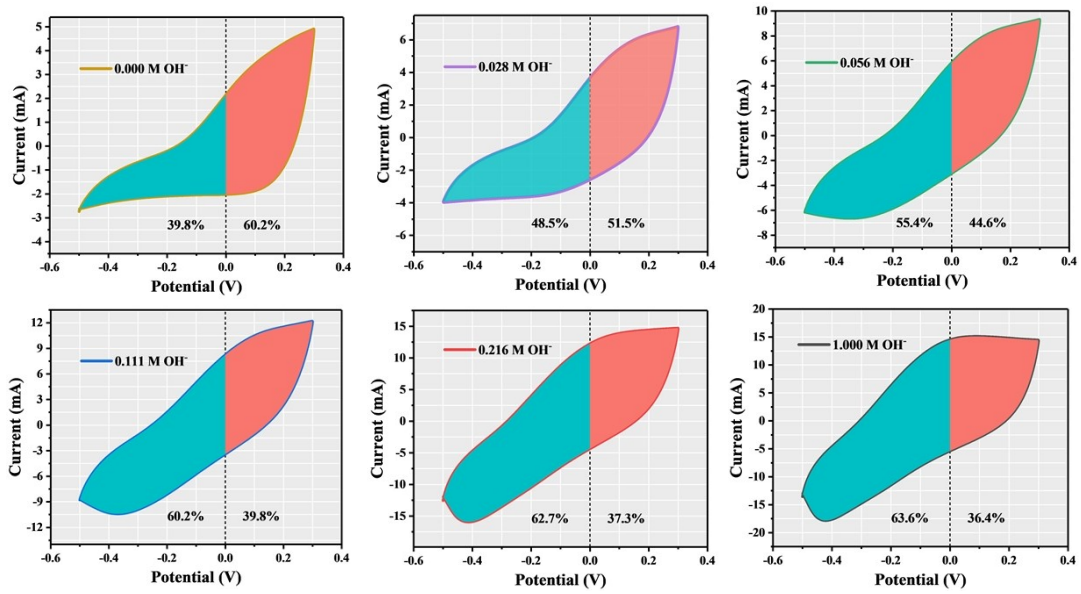

Fig.S9. Percentage of CV area between positive and negative potentials at different OH^- concentrations.

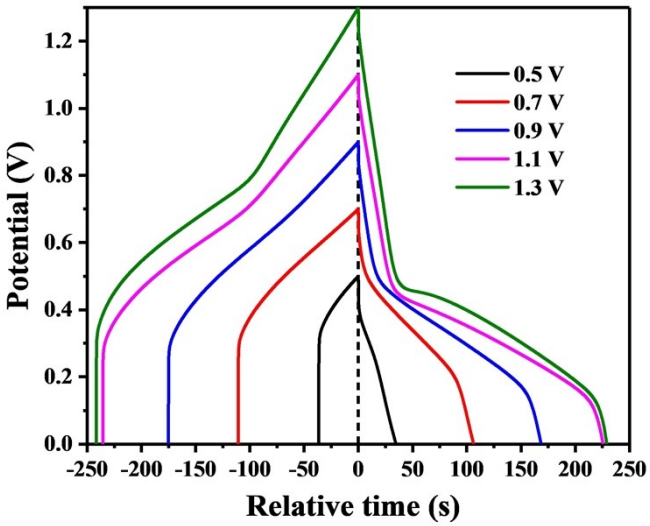

Fig.S10. Galvanostatic current charge/discharge curves of M-300//H-$NiCo_2O_4$ asymmetrical supercapacitor under different potential windows.

Table S5. Specific capacitance of M-300//H-$NiCo_2O_4$ asymmetrical supercapacitor under various current densities.

Current density (A g^{-1})	1.0	2.0	3.0	5.0	7.0	10.0
Specific capacitance (F g^{-1})	207.5	181.3	160.6	133.6	111.4	98.2

Table S6. Power density and energy density of M-300/H-$NiCo_2O_4$ and related reports.

Device	Power density (W kg^{-1})	Energy density (Wh kg^{-1})	Ref.
PMCHC//$W_{0.4}Mo_{0.6}O_3$	750.5	20.2	[68]
	7481.8	15.4	
U-3DHPC//U-3DHPC	200.7	19.2	[67]
	4000	10.6	
$LiCoPO_4$//$FeVO_4$	484	27	[69]
	737	26	
	1010	23	
	1326	21	
G@MnO_2//Gr	197.0	30.6	[8]
	11,804	7.9	
M-300//H-$NiCo_2O_4$	550	34.9	This work
	1100	30.5	
	1650	27.0	
	2750	22.5	
	3850	18.7	
	5500	16.5	

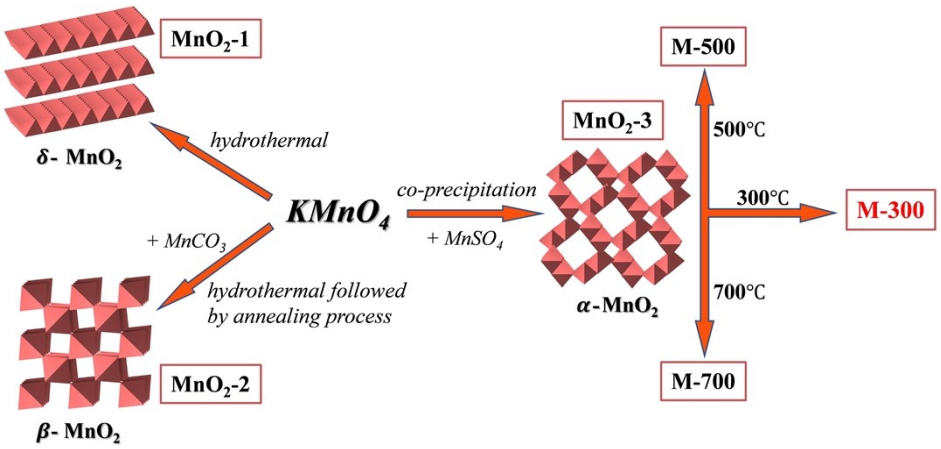

Fig.S11. Schematic diagram of the synthesis of all samples

Table S7. The areal mass loading of active material of all samples.

Sample	MnO_2-1	MnO_2-2	MnO_2-3	M-300	M-500	M-700
Areal mass (mg cm^{-2})	2.50	3.70	3.56	2.00	2.54	3.49

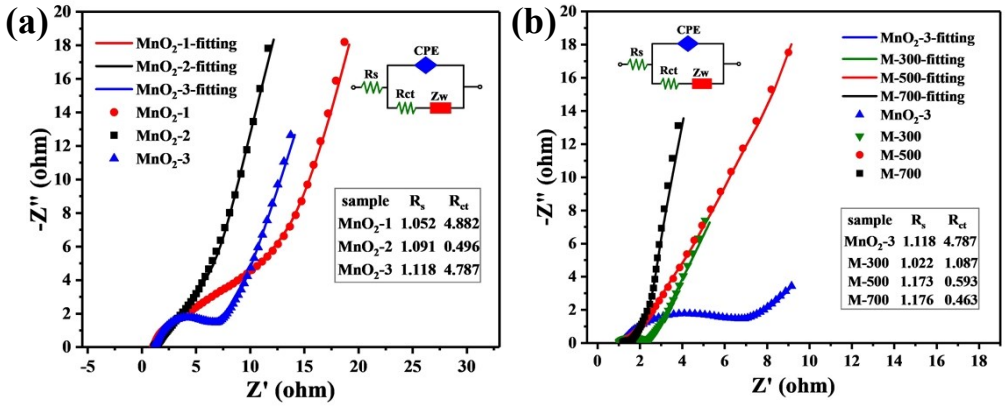

Fig.S12. EIS curve fitting results of (a) MnO_2-1, MnO_2-2 and MnO_2-3; (b) MnO_2-3, M-300, M-500 and M-700.

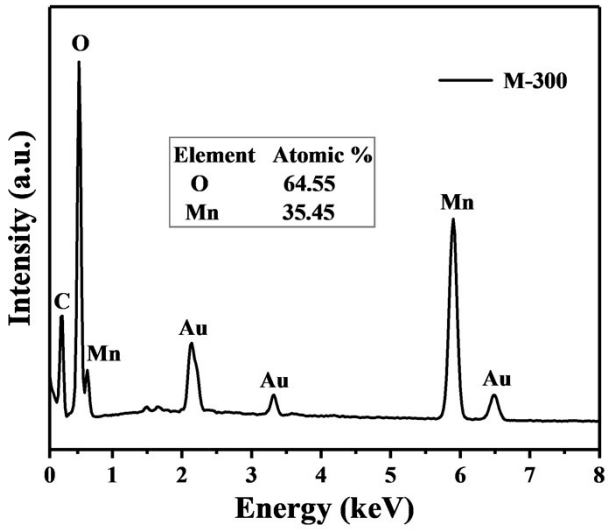

Fig.S13. EDS images of M-300.